AIP | Journal of Applied Physics

Enhanced photoluminescence from zinc oxide by plasmonic resonance of reduced graphene oxide

Kukjoo Kim, Seong Min Lee, Yun Seon Do, Sung Il Ahn, and Kyung Cheol Choi

Citation: Journal of Applied Physics **114**, 074903 (2013); doi: 10.1063/1.4818953
View online: http://dx.doi.org/10.1063/1.4818953
View Table of Contents: http://scitation.aip.org/content/aip/journal/jap/114/7?ver=pdfcov
Published by the AIP Publishing

Enhanced photoluminescence from zinc oxide by plasmonic resonance of reduced graphene oxide

Kukjoo Kim,[1,a)] Seong Min Lee,[1,a)] Yun Seon Do,[1] Sung Il Ahn,[2] and Kyung Cheol Choi[1,b)]
[1]*Department of Electrical Engineering, Korea Advanced Institute of Science and Technology (KAIST), 291 Daehak-ro, Yuseong-gu, Daejeon 305-701, South Korea*
[2]*Department of Engineering in Energy and Applied Chemistry, Silla University, 140 Baegyang-daero 700beon-gil, Sasang-gu, Busan 617-736, South Korea*

(Received 1 July 2013; accepted 5 August 2013; published online 20 August 2013)

We demonstrate 2.79- and 10.16-fold enhanced photoluminescence (PL) from band-edge and defect levels of zinc oxide (ZnO) using a plasmonic resonance of reduced graphene oxide (RGO) in the UV frequency range. RGO shows superior tunability on the light absorption of ZnO by the confined plasmonic resonance, which results in strong PL emission. We conclude that the absorption of ZnO in close proximity to the RGO layer can be enhanced. These arguments are strongly supported by different PL enhancements depending on the distance between RGO and ZnO layers, time-resolved PL, and numerical calculations. © *2013 AIP Publishing LLC*. [http://dx.doi.org/10.1063/1.4818953]

I. INTRODUCTION

Graphene, a single layer of carbon atoms with a two-dimensional honeycomb structure, has attracted a considerable amount of interest from optoelectronic and material scientists since its practical discovery.[1,2] Much effort has been dedicated to investigate and exploit its unique properties, such as high electrical[3,4] and thermal[5] conductivity, excellent mechanical strength[6] in flexible and stretchable applications, high surface area,[7,8] and ability to serve as a gas barrier.[9] One intriguing property of graphene is its plasmonic behavior similar to that of metals. Because similar characteristics of metal have been conventionally utilized to affect and eventually to enhance the emission from various light emitters, the plasmonic behavior of graphene is a very interesting research area for those studying highly efficient optoelectronic devices.

Recently, Hwang *et al.*[10] associated graphene plasmons with enhanced light emission from zinc oxide (ZnO), a typical light emitting material. Studies of the light emission from ZnO adopting metallic nanostructures such as Ag gratings,[11] Au-coated films,[12] Pt composites,[13] and Al/AlOx coated layers[14] commonly utilize the surface plasmons (SPs) of these types of metals. Accordingly, it is feasible to associate graphene plasmons with the enhanced emission of ZnO. However, further investigation is required, as research on graphene plasmons is at an early stage, like most research on graphene. Therefore, the mechanism of enhanced emission by graphene plasmons has not yet been thoroughly revealed. In addition, most of works thus far have dealt with non-scalable and expensive production methods pertaining to graphene, such as mechanical exfoliation and chemical vapor deposition. This has exposed a critical limit as regards applicability to practical devices.

In this report, we demonstrate the use of solution-processed graphene oxide (GO) and reduced graphene oxide (RGO) for the enhanced light emission from ZnO as a large-scale and cost-effective method. While graphene by means of mechanical exfoliation induces unique graphene plasmons similar to those of metals,[10] this work reports that chemically reduced GO can induce a plasmonic resonance which is localized around flakes of RGO, fairly analogous to SPs of metallic nanoparticles or nanostructures. 2.79- and 10.16-fold enhanced photoluminescence (PL) from band-edge and defect levels of ZnO are obtained using the plasmonic resonance of RGO in the UV frequency domain. We conclude that the absorption of ZnO in close proximity to the RGO layer can be enhanced. These arguments are strongly supported by different PL enhancements depending on the distance between RGO and ZnO layers, time-resolved PL (TRPL), and numerical calculations. The enhanced light emission of ZnO and the mechanism underneath are also verified completely by steady PL and TRPL measurements with a subsequent in-depth discussion, thus realizing a great advance in the possibility of applying graphene in optoelectronic devices.

II. EXPERIMENTAL DETAILS

GO was prepared using a modified Hummers method, as reported elsewhere[15] (for the detailed process, see supplementary material[16]). The prepared aqueous GO solution was dispensed on precleaned Si wafers or quartz substrates, allowed to spread for 1 min, and then spin-coated at 2000 rpm for 1 min. The spin speed was slowly increased to the maximum speed at an acceleration rate of 200 rpm/s to obtain uniform GO films. The resulting films were dried in a vacuum oven at 80 °C for 30 min. The RGO films were obtained by hydrazine vapor reduction using a method reported in the literature.[17–20] Samples were put in a glass Petri dish and heated to 90 °C, after which a few drops of hydrazine monohydrate ($N_2H_4 \cdot H_2O$, 80%, Samchun Chemical) were dispensed beside the samples. The Petri dish was then

[a)]K. Kim and S. M. Lee contributed equally to this work.
[b)]Author to whom correspondence should be addressed. Electronic mail: kyungcc@kaist.ac.kr.

sealed by winding Teflon tape around the dish and the cover. The reduction process lasted 4 h. The RGO samples were dried overnight in a vacuum oven at 80 °C. Magnesium oxide (MgO) as a dielectric spacer was deposited with various thicknesses at 60 °C by means of electron beam evaporation. Then, 100 nm-thick ZnO films were deposited by means of atomic layer deposition (ALD) at 250 °C.

GO flakes and film morphology were analyzed by atomic force microscopy (AFM, XE-100, Park Systems). The extinction spectra of GO and RGO were measured by a Shimadzu UV-Vis spectrophotometer (UV-2550, Japan). PL emission spectra were recorded with a Hitachi fluorescence spectrophotometer (F-7000, Japan) equipped with a Xe lamp using a reflective configuration. In our experiment, a continuous-wave (CW) 325 nm light from a Xe lamp was used for the optical excitation of ZnO. The excitation light was illuminated onto the ZnO side with an incident angle of 60° against the normal direction. The X-ray diffraction (XRD) spectra of ZnO were obtained by a thin-film X-ray diffractometer (Rigaku D/MAX-RC) using graphite-monochromatized Cu Kα radiation at 40 kV and 100 mA. To examine the reduction of GO to RGO, an X-ray photoelectron spectroscopy (XPS) analysis was performed by a Sigma probe X-ray photoelectron spectrometer (Thermo V.G. Scientific). The Raman spectra of GO and RGO were obtained with a high-resolution, dispersive Raman spectrometer system (Horiba-Jobin Yvon, LabRam-HR) with 514 nm Ar CW laser excitation. The TRPL was measured by a fluorescence spectrometer (Horiba Jobin Yvon FL3-2IHR) equipped with a 265 nm light-emitting diode source (NanoLED-265) and a Symphony linear InGaAs array detector (IGA-512X1-50-1700-1LS).

III. RESULTS AND DISCUSSION

Fig. 1(a) shows a graphical representation of the hybrid structure consisting of ZnO as a light emitter, a dielectric spacer, and an RGO layer on a Si wafer. In this work, we examined both solution-processed pristine GO and hydrazine vapor reduced RGO. RGO is known to be more similar to pristine graphene than GO. Considering that the absorption band of ZnO is positioned in the UV regime, we used the localized plasmonic resonance of GO and RGO, which can cause strong light absorption of ZnO in the UV region. In the above structure, the ZnO is 100 nm thick. As shown in Figs. 1(b) and 1(c), the GO layer consists of numerous flakes (<5 μm) which are randomly stacked by means of spin-coating. The measured thickness of the GO layer was approximately 20 nm according to AFM measurements. To verify the plasmonic effect, we applied MgO as a means of controlling the distance between the plasmonic resonance center and the light emitter.

XPS and Raman spectroscopy were conducted to investigate the degree of reduction of RGO as reported elsewhere[21,22] (for the Raman spectra, see supplementary material, Fig. S2[16]). Fig. 1(d) shows the C1s XPS spectra of the GO and RGO samples with deconvoluted curve fits. Deconvolution revealed there are three main sub-peaks originating from C-C, C-O, and C=O centered approximately at 284.8, 286.9, and 288.2 eV, respectively. Unlike the C-C peak, the intensities of the C-O and C=O peaks decrease significantly after hydrazine vapor reduction, indicating that numerous oxygen atoms were removed from the RGO sample. Fig. 1(e) shows the extinction spectra of GO and RGO, representing distinct light absorption in the UV regime. UV-graded quartz was used for baseline calibration, and the

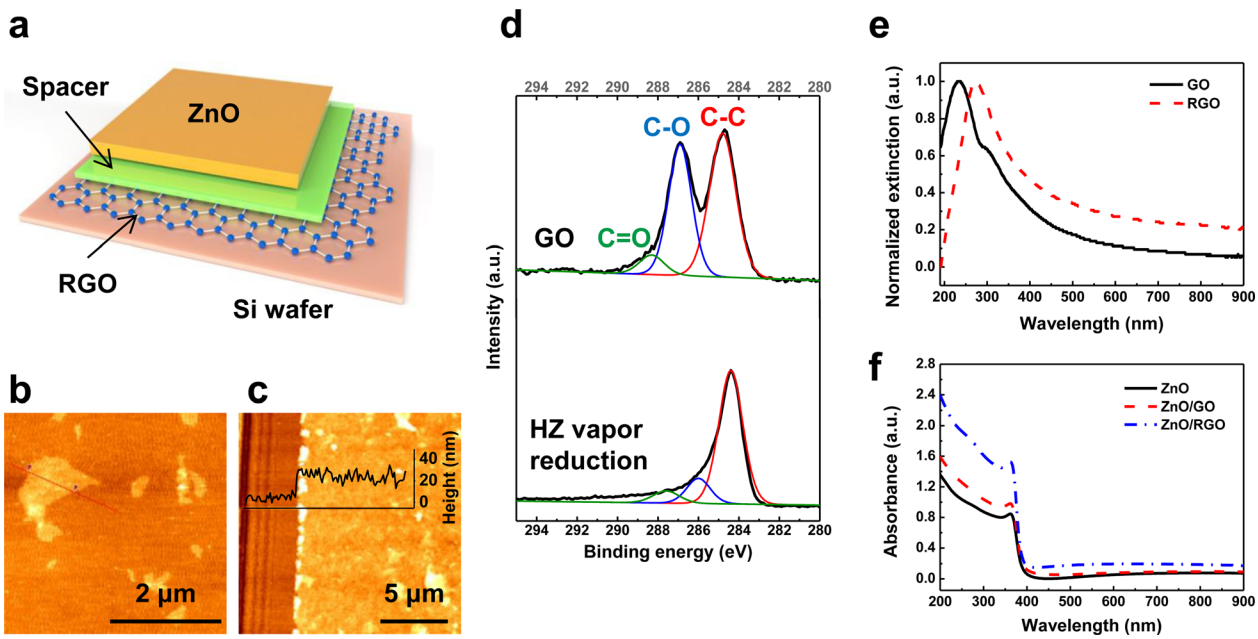

FIG. 1. (a) Schematic illustration of the hybrid structure of ZnO and RGO layers. MgO was selected as a dielectric spacer for the investigation of the plasmonic effect on the distance. (b) AFM image of prepared GO flakes on a Si wafer substrate. (c) AFM image of a spin-coated GO film scratched by a surgical blade. The average height of the GO layer is approximately 20 nm. (d) Curve fit of C1s XPS spectra of GO and RGO on a Si wafer substrate. Hydrazine (HZ) vapor reduction was applied to obtain RGO. (e) Normalized extinction spectra of GO and RGO on UV-graded quartz substrates. (f) Absorbance spectra of ZnO, ZnO/GO, and ZnO/RGO films on UV-graded quartz substrates.

extinction spectrum at each sample was normalized by respective peak intensities. This strong absorption in UV region is ascribed to the localized plasmonic resonance of GO and RGO consisting of many flakes. The GO and RGO samples showed maximum peak intensities at 235 and 273 nm, respectively. The reduction of GO resulted in a red-shift of the plasmonic resonance. With this shift, the plasmonic resonance of RGO showed a better fit to the absorption band of ZnO compared to that of GO. Fig. 1(f) shows the total absorbance in the bilayer structures of ZnO/GO and ZnO/RGO, in contrast to that of bare ZnO film on quartz substrates. ZnO incorporating RGO shows stronger absorption in the UV region as a result of the plasmonic resonance.

Fig. 2(a) shows the entire PL spectra from ZnO, ZnO/GO, and ZnO/RGO samples under irradiation with a 325 nm CW Xe lamp. According to previous reports, ZnO shows UV emission around 380 nm and a broad visible emission, as characterized by the band-edge and structural defects of ZnO, respectively.[23–25] In our experiment, in which ZnO was fabricated by ALD, the band-edge and defect level emission of ZnO appeared at 380 nm and 525 nm, respectively. As shown in Fig. 2(a), the emission intensity from ZnO with GO and RGO is higher than that of the ZnO-only sample. In addition, RGO showed a larger enhancement of PL from ZnO than GO did. Meanwhile, weak bumps were observed at around 360 nm after introducing the GO and RGO due to the intrinsic PL emission of GO and RGO. Although perfect graphene commonly has a zero bandgap, GO and RGO are known for showing UV light emission arising from the energy bandgap,[26] as shown in Fig. 2(b). Therefore, to determine the exact emission from ZnO, we eliminated the emissions of GO and RGO from the raw PL spectra of the fully fabricated structure by subtracting the intrinsic emission from GO and RGO. Because the PL spectrum of graphene is positioned in the lower wavelength region, we assumed that the emissions of GO (or RGO) can be linearly subtracted from the total PL spectrum to obtain the pure PL spectrum of ZnO. Fig. 2(c) shows the corrected PL emission intensity of ZnO. The PL spectra of ZnO with the existence of GO and RGO show the same tendency with those in Fig. 2(a), even after the subtraction of the inherent PL emission of GO and RGO. In addition to the band-edge emission, it is noteworthy that the defect-level emission from ZnO also increased. This indicates that the absorption of ZnO is enhanced with the aid of GO and RGO because the modification of radiative transition rates or emission rates, which is another process of the PL emission, will induce an enhancement in a specific narrow band.

We calculated the enhancement factor of the PL emission based on integration in the following ranges: (1) from 360 to 420 nm for the band-edge emission; (2) from 420 to 650 nm for the defect-level emission. As shown in Fig. 2(d), enhancement factors were plotted in terms of the absorbance of ZnO, ZnO/GO, and ZnO/RGO at the excitation wavelength (325 nm) which can be obtained from Fig. 1(f). Enhancement was simultaneously achieved at two radiation bands. In the band-edge emission, 1.37- and 2.79-fold enhancements by GO and RGO were obtained, respectively. In the defect-level emission, 1.74- and 10.16-fold enhancements by GO and RGO were obtained, respectively. The larger enhancement of the PL emission from the RGO-incorporated sample for both radiation bands compared to the GO-incorporated sample implies the intensified excitation of the ZnO film by the plasmonic resonance of RGO.

According to previous reports, plasmonic resonances can affect light emitters in both processes of absorption and emission.[27–30] In other words, plasmonic resonances can enhance either the absorption rate or the radiative decay rate of a specific light emitter. Whether the plasmon has an effect on absorption or emission can be assessed by several

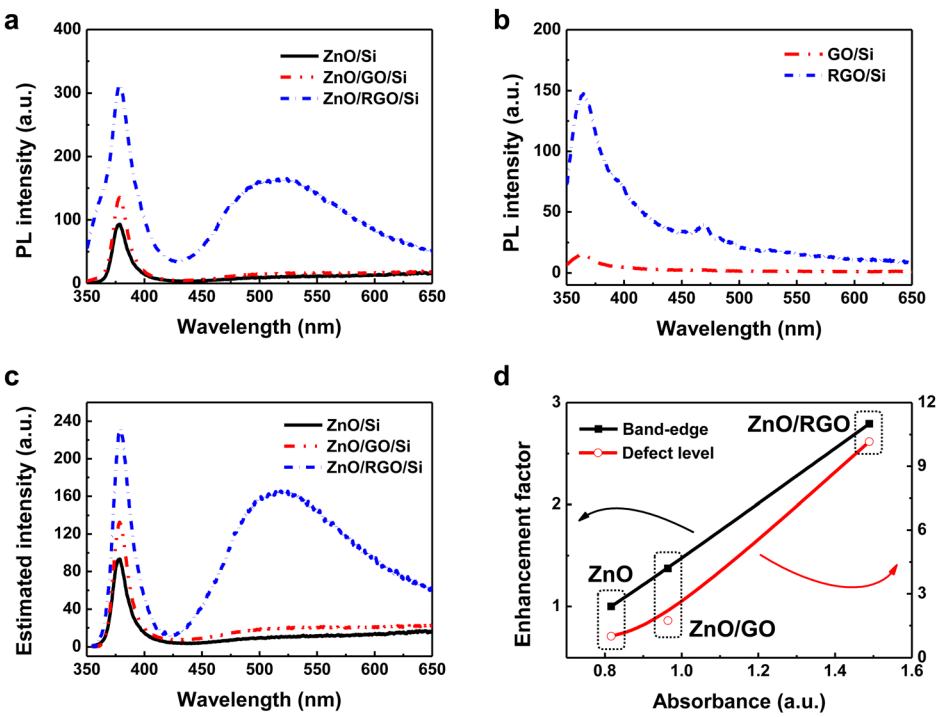

FIG. 2. (a) Raw PL spectra from the ZnO, ZnO/GO, and ZnO/RGO samples on Si wafers measured under a reflective configuration at room temperature. (b) Intrinsic PL spectra from the GO and RGO on a Si wafer. (c) Corrected PL spectra of ZnO, ZnO/GO, and ZnO/RGO samples without bump peaks originating from intrinsic PL of GO and RGO. (d) PL enhancement factors of the band-edge and defect level emissions for ZnO, ZnO/GO, and ZnO/RGO samples upon the partial integration of the emission spectra. X-axis indicates the absorbance of each sample at the excitation wavelength (325 nm).

measurements. Fig. 3(a) shows measured PL spectra of RGO-incorporated ZnO films with and without MgO spacer layers between ZnO and RGO layers. The correction of the PL spectra was carried out in the same manner as was in Fig. 2(c). The plasmonic effect of RGO, and eventually the PL intensity of ZnO, was altered by introducing spacer layers with various thicknesses. The spacer thickness was varied as 10, 20, and 30 nm. The inset of Fig. 3(a) shows the PL intensities integrated from 355 to 425 nm and plotted according to the spacer thickness. The lower PL intensity of the samples with the thicker spacer indicates a weaker plasmonic effect of RGO. Furthermore, the PL intensity monotonically decreases as the distance between the ZnO and RGO layers increases. This is direct evidence to support that the plasmonic resonance of RGO is affecting the absorption of ZnO. If the plasmon is related to the radiative decay or emission process of ZnO, we should be able to find an optimum spacer thickness other than zero where the PL intensity reaches its maximum by minimizing the quenching of excitons.

By measuring the radiative decay time or TRPL, one can also distinguish whether the plasmonic resonance is affecting the absorption or the emission of a specific light emitter because the latter case will induce a shorter lifetime of the excitons. Fig. 3(b) shows the TRPL results of ZnO, ZnO/GO, ZnO/RGO, and ZnO/spacer/RGO samples with the inherent system decay. There were no significant differences in the decay tendencies of each sample. The decay time remained almost constant regardless of the existence of GO, RGO, or the dielectric spacer, implying that the plasmonic resonance from RGO influences not the emission but the absorption of ZnO.

On the other hand, localized SPs are known to result in strong field confinement around metallic nanostructures in the resonance wavelength. Thus, local field enhancement can be an analytic probe for the detection of a plasmonic resonance. To understand the PL enhancement originating from the plasmonic effect, we analyzed the local field distribution at a wavelength of 325 nm by the three-dimensional finite-difference time-domain (FDTD) method (FDTD solutions, Lumerical Solutions, Inc., Canada). Fig. 3(c) shows the simulation configuration. Based on the AFM images in Fig. 1, an RGO flake was modeled as a cylinder (with a radius of 200 nm and a thickness of 20 nm) and was positioned on the Si wafer. A ZnO layer of 120 nm was positioned on top of cylindrical RGO. Fig. 3(d) shows the calculated electric field distributions for the ZnO-only case and for ZnO/RGO case on Si wafers.

As shown in Fig. 3(d), the electric field in the ZnO layer at the excitation wavelength (325 nm) was intensified by the existence of RGO compared to the field of ZnO-only case and was strongly confined near the RGO flake. In addition, the field distribution coincides well with that of ZnO with Ag, a well-known plasmonic metal, although the amount of the enhancement is smaller (see supplementary material, Fig. S4[16]). Furthermore, the degree of the enhancement of the field intensity decreased as the spacer became thicker, thus showing good agreement with the PL results in Fig. 3(a) (see supplementary material, Fig. S4 and Table S1[16]).

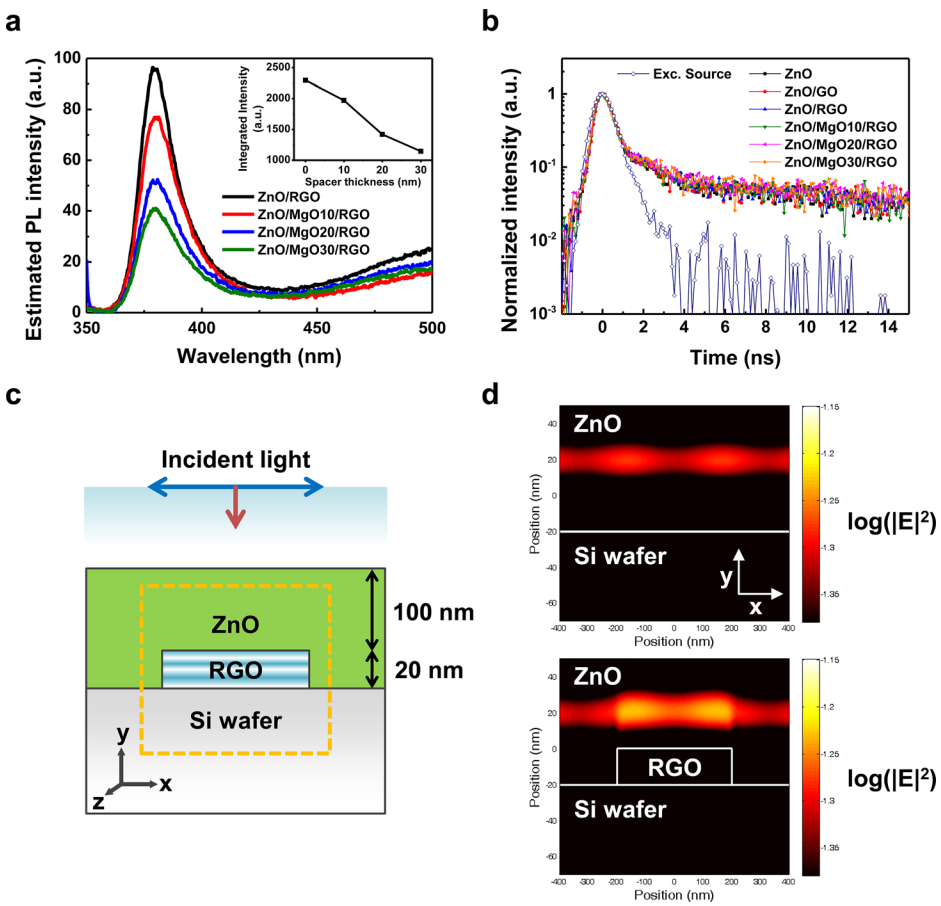

FIG. 3. (a) Corrected PL spectra of RGO-incorporated samples according to the various spacer thicknesses. Inset shows integrated PL intensities of identical samples from 355 to 425 nm. (b) Time-resolved PL intensities for different spacer thicknesses (0, 10, 20, and 30 nm) with 266 nm excitation. (c) Calculation configuration for the electric field distribution around the ZnO layer on the cylindrical RGO structure. Plane wave is illuminated at normal incidence with x-direction linear polarization. (d) Calculated electric field intensities ($\log(|E|^2)$) on the x-y plane at the excitation wavelength, showing the ZnO layer with and without the RGO cylinder.

This result is solid evidence of the detection of the plasmonic resonance caused by RGO. Therefore, based on the FDTD calculations, we conclude that RGO induces a local field enhancement in the absorption band of ZnO that is similar to the effect of the metal-induced plasmons but somewhat weaker.

We believe the increased absorption of ZnO under UV light irradiation leads to strong emission from ZnO. The localized plasmonic oscillation driven by GO and RGO in the UV frequency domain causes strong absorption of UV light in the ZnO layer. After the reduction of GO, the peak of its plasmon-band moved to a longer wavelength, resulting in deep spectral overlap with the absorption band of ZnO. This is in good agreement with the PL results of ZnO on the RGO film, which showed higher intensity than that of ZnO on GO film. Also, the two radiation bands (the band-edge and defect level) of ZnO increased together in our results. Thus, the enhancement in this work is attributed to the enhanced absorption of ZnO and not to the Purcell effect owing to the spectral overlap between the SP resonance and the radiative transition.[31,32] In addition, these arguments are strongly supported by the fact that the decay time remained constant in the TRPL measurements despite the great increase in the emission intensity. The constant decay time implies the invariance of the Purcell factor in light emitting materials.[33] The fact that the PL intensity decreased as the distance between the ZnO and RGO layers increased also indicates the resonant excitation of ZnO by the RGO layer becomes weaker with a thicker spacer.

IV. CONCLUSION

In conclusion, we demonstrated the use of chemically derived graphene prepared by a solution process. Plasmonic spectral tuning of the PL emission from ZnO thin films was examined exploiting GO and RGO under UV light irradiation. The RGO showed better performance to improve the light emission from the band-edge and defect levels of ZnO compared to the case of GO. The observed enhancement in the PL was attributed to the increased absorption of ZnO affected by the plasmonic oscillation of RGO. According to our results, the amount of the PL enhancement by RGO is comparable to the findings of reports using mechanically exfoliated single layer graphene sheets. This suggests that solution-processed graphene can be used in numerous large-scale, low-cost, and highly efficient optoelectronic devices.

ACKNOWLEDGMENTS

This work was supported by the National Research Foundation of Korea (NRF) grant funded by the Korea government (MSIP) (CAFDC/Kyung Cheol Choi/No. 2007-0056090) and was also supported by Basic Science Research Program through the NRF funded by the Ministry of Education, Science and Technology (No. 2012R1A1A2006729).

[1]K. S. Novoselov, A. K. Geim, S. V. Morozov, D. Jiang, Y. Zhang, S. V. Dubonos, I. V. Grigorieva, and A. A. Firsov, Science **306**, 666 (2004).
[2]K. S. Novoselov, D. Jiang, F. Schedin, T. J. Booth, V. V. Khotkevich, S. V. Morozov, and A. K. Geim, Proc. Natl. Acad. Sci. U.S.A. **102**, 10451 (2005).
[3]K. S. Kim, Y. Zhao, H. Jang, S. Y. Lee, J. M. Kim, K. S. Kim, J.-H. Ahn, P. Kim, J.-Y. Choi, and B. H. Hong, Nature (London) **457**, 706 (2009).
[4]S. Bae, H. Kim, Y. Lee, X. Xu, J.-S. Park, Y. Zheng, J. Balakrishnan, T. Lei, H. Ri Kim, Y. I. Song, Y.-J. Kim, K. S. Kim, B. Ozyilmaz, J.-H. Ahn, B. H. Hong, and S. Iijima, Nat. Nanotechnol. **5**, 574 (2010).
[5]A. A. Balandin, S. Ghosh, W. Bao, I. Calizo, D. Teweldebrhan, F. Miao, and C. N. Lau, Nano Lett. **8**, 902 (2008).
[6]C. Lee, X. Wei, J. W. Kysar, and J. Hone, Science **321**, 385 (2008).
[7]H. K. Chae, D. Y. Siberio-Pérez, J. Kim, Y. Go, M. Eddaoudi, A. J. Matzger, M. O'Keeffe, and O. M. Yaghi, Nature (London) **427**, 523 (2004).
[8]V. Dua, S. P. Surwade, S. Ammu, S. R. Agnihotra, S. Jain, K. E. Roberts, S. Park, R. S. Ruoff, and S. K. Manohar, Angew. Chem. **122**, 2200 (2010).
[9]H. Kim, Y. Miura, and C. W. Macosko, Chem. Mater. **22**, 3441 (2010).
[10]S. W. Hwang, D. H. Shin, C. O. Kim, S. H. Hong, M. C. Kim, J. Kim, K. Y. Lim, S. Kim, S.-H. Choi, K. J. Ahn, G. Kim, S. H. Sim, and B. H. Hong, Phys. Rev. Lett. **105**, 127403 (2010).
[11]M. Gwon, E. Lee, D.-W. Kim, K.-J. Yee, M. J. Lee, and Y. S. Kim, Opt. Exp. **19**, 5895 (2011).
[12]Y. Zhang, X. Li, and X. Ren, Opt. Exp. **17**, 8735 (2009).
[13]J. M. Lin, H. Y. Lin, C. L. Cheng, and Y. F. Chen, Nanotechnology **17**, 4391 (2006).
[14]W. H. Ni, J. An, C. W. Lai, H. C. Ong, and J. B. Xu, J. Appl. Phys. **100**, 026103 (2006).
[15]W. S. Hummers and R. E. Offeman, J. Am. Chem. Soc. **80**, 1339 (1958).
[16]See supplementary material at http://dx.doi.org/10.1063/1.4818953 for details of the preparation of GO and RGO; Raman, XRD, and FDTD simulation results.
[17]S. Gilje, S. Han, M. Wang, K. L. Wang, and R. B. Kaner, Nano Lett. **7**, 3394 (2007).
[18]S. Park, Y. Hu, J. O. Hwang, E.-S. Lee, L. B. Casabianca, W. Cai, J. R. Potts, H.-W. Ha, S. Chen, J. Oh, S. O. Kim, Y.-H. Kim, Y. Ishii, and R. S. Ruoff, Nat. Commun. **3**, 638 (2012).
[19]G. Eda, G. Fanchini, and M. Chhowalla, Nat. Nanotechnol. **3**, 270 (2008).
[20]C. Gómez-Navarro, R. T. Weitz, A. M. Bittner, M. Scolari, A. Mews, M. Burghard, and K. Kern, Nano Lett. **7**, 3499 (2007).
[21]S. Stankovich, D. A. Dikin, R. D. Piner, K. A. Kohlhaas, A. Kleinhammes, Y. Jia, Y. Wu, S. T. Nguyen, and R. S. Ruoff, Carbon **45**, 1558 (2007).
[22]D. Yang, A. Velamakanni, G. Bozoklu, S. Park, M. Stoller, R. D. Piner, S. Stankovich, I. Jung, D. A. Field, C. A. Ventrice, Jr., and R. S. Ruoff, Carbon **47**, 145 (2009).
[23]M. S. Kim, G. Nam, S. Kim, D. Y. Kim, D.-Y. Lee, J. S. Kim, S.-O. Kim, J. S. Kim, J.-S. Son, and J.-Y. Leem, J. Lumin. **132**, 2581 (2012).
[24]R. F. Haglund, Jr., B. J. Lawrie, and R. Mu, Thin Solid Films **518**, 4637 (2010).
[25]D. J. Gargas, H. Gao, H. Wang, and P. Yang, Nano Lett. **11**, 3792 (2011).
[26]G. Eda, Y. Lin, C. Mattevi, H. Yamaguchi, H. Chen, I. Chen, C. Chen, and M. Chhowalla, Adv. Mater. **22**, 505 (2010).
[27]D. A. Weitz, S. Garoff, C. D. Hanson, T. J. Gramila, and J. I. Gersten, J. Lumin. **24/25**, 83 (1981).
[28]K. Aslan, M. J. R. Previte, Y. Zhang, and C. D. Geddes, J. Phys. Chem. C **112**, 18368 (2008).
[29]J. B. Khurgin, G. Sun, and R. A. Soref, Appl. Phys. Lett. **94**, 071103 (2009).
[30]G. Sun, J. B. Khurgin, and R. A. Soref, Appl. Phys. Lett. **94**, 101103 (2009).
[31]S. M. Lee, D. Kim, D. Y. Jeon, and K. C. Choi, Small **8**, 1350 (2012).
[32]K. H. Cho, S. I. Ahn, S. M. Lee, C. S. Choi, and K. C. Choi, Appl. Phys. Lett. **97**, 193306 (2010).
[33]B. J. Lawrie, R. F. Haglund, Jr., and R. Mu, Opt. Exp. **17**, 2565 (2009).